Supplement of Atmos. Meas. Tech., 9, 2497–2534, 2016
http://www.atmos-meas-tech.net/9/2497/2016/
doi:10.5194/amt-9-2497-2016-supplement

Atmospheric Measurement Techniques
Open Access
EGU

Supplement of

Ground-based assessment of the bias and long-term stability of 14 limb and occultation ozone profile data records

Daan Hubert et al.

Correspondence to: D. Hubert (daan.hubert@aeronomie.be)

Contents

This document contains following supplementary figures which could not be shown in the main manuscript due to space limitations.

- Fig. S1: latitude-time cross section of the co-location samples used in the analysis.
- Fig. S2: vertical profile of drift uncertainty adjustment factor κ for ozonesonde and lidar networks, and all satellite records.
- Fig. S3: sensitivity of the network-averaged drift results to several regression analysis parameters.
- Fig. S4: sensitivity of the network-averaged drift results to selection of ground sites.
- Fig. S5–S18: bias, comparison spread and network-averaged drift results in four ozone profile representations. One figure per satellite record; results are split up per type of correlative instrument and latitude band to allow a more quantitative reading of the results.
- Fig. S19: bias relative to ozonesonde and lidar of sunrise and sunset observations by solar occultation instruments.
- Fig. S20: month-dependence of the bias and comparison spread of seven sounders relative to Arctic ozonesondes.

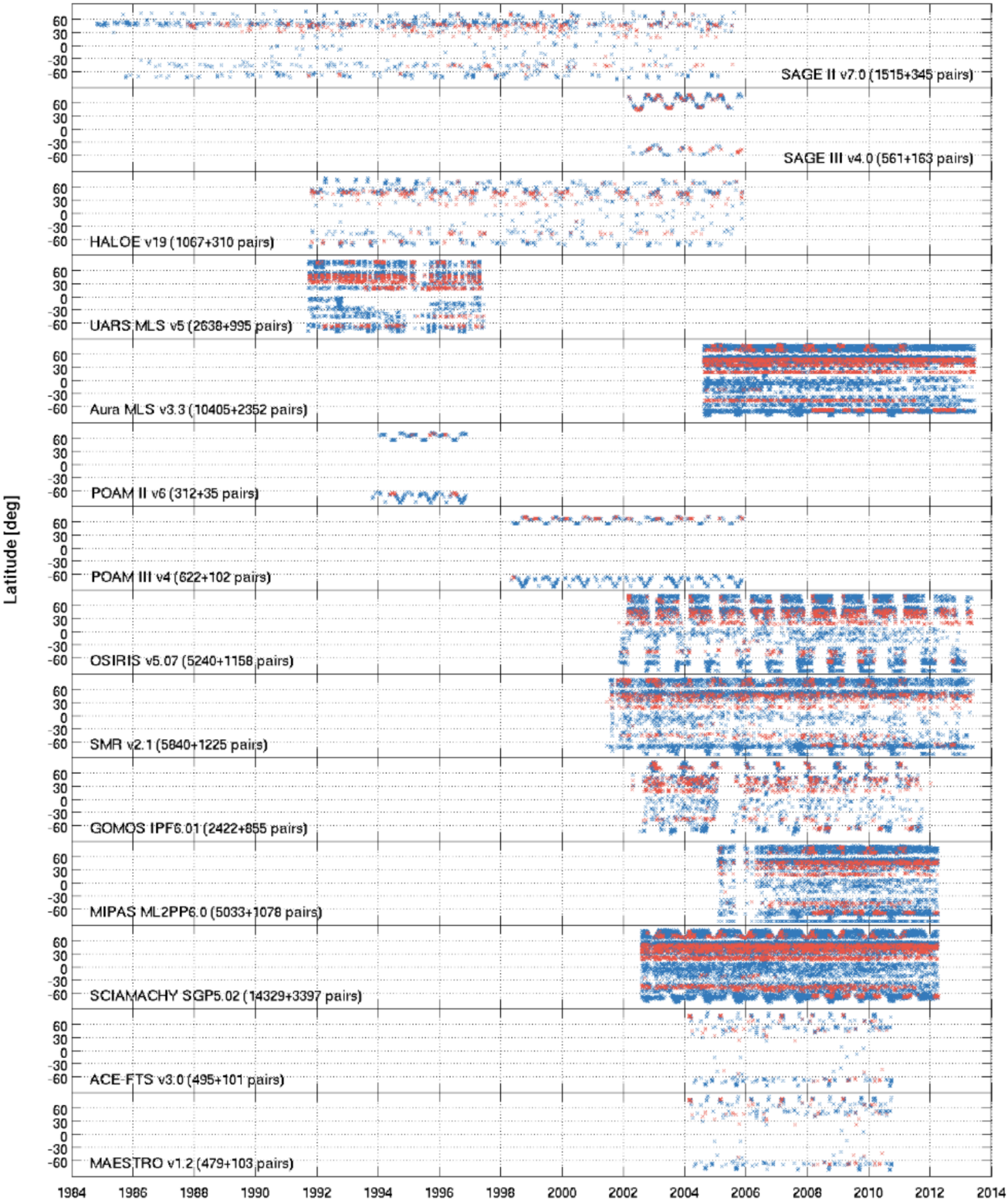

Figure S1. Latitude-time cross section of the co-locations of NDACC/GAW/SHADOZ ozonesonde (blue) and NDACC stratospheric ozone lidar (red) with fourteen limb/occultation ozone profile records. Latitude and time correspond to that of satellite profile. Total number of co-locating pairs for sonde and lidar are mentioned separately between brackets.

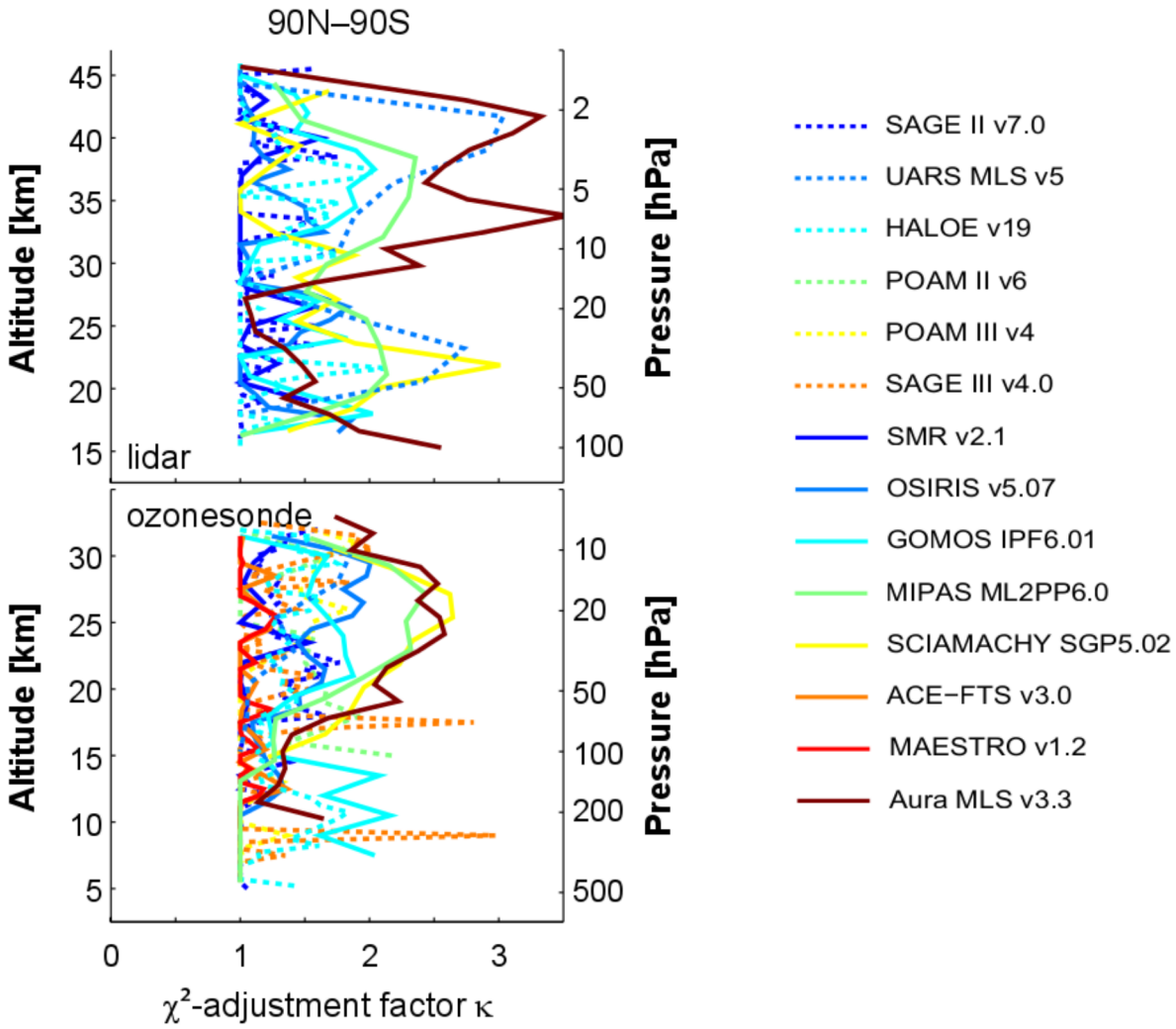

Figure S2. Adjustment factor □ to incorporate unaccounted for sources of uncertainty (sampling, ground-network homogeneity, ...) in the estimation of network-averaged drift of limb/occultation ozone profile data relative to lidar (top) and ozonesonde (bottom) measurements. See Sect. 4.1.2 for more details.

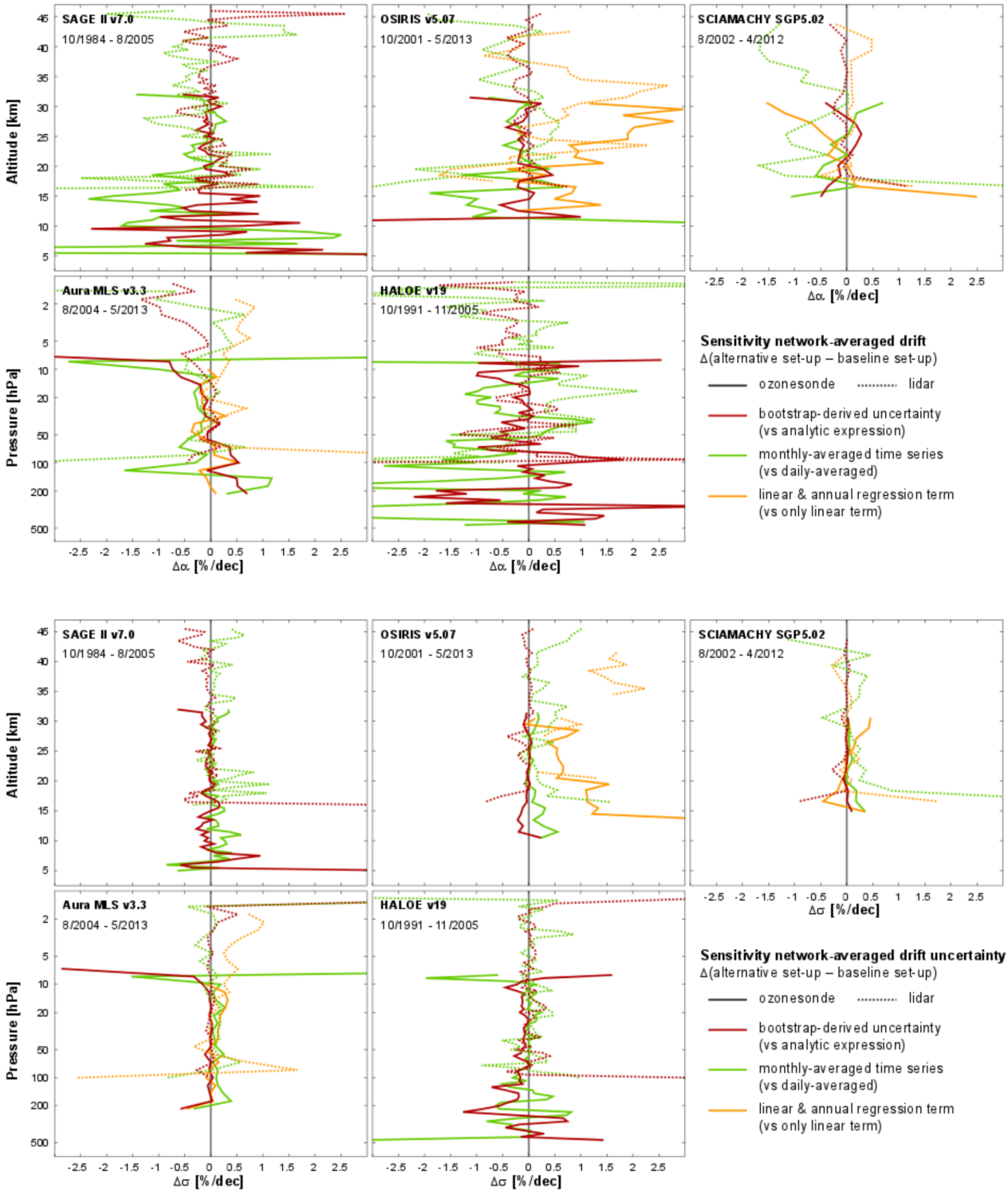

Figure S3. Sensitivity of ozonesonde and lidar network-averaged drift 布(top part) and one sigma uncertainty 澳(bottom part) to several regression analysis parameters (cfr. Sec. 4.1.3). Shown is the difference of an alternative minus the baseline regression set-up for five satellite records. Three alternatives are depicted: (a) uncertainties derived from bootstrap (red) instead of analytic expression, (b) regression of monthly-averaged comparison timeseries (green) instead of daily-averaged, and, (c) regression model with linear and annual terms (yellow) instead of only linear term. Larger differences appear for the latter set-up since only timeseries with a significant annual cycle are regressed, hence leading to a quite different sample of timeseries included in the network-averages.

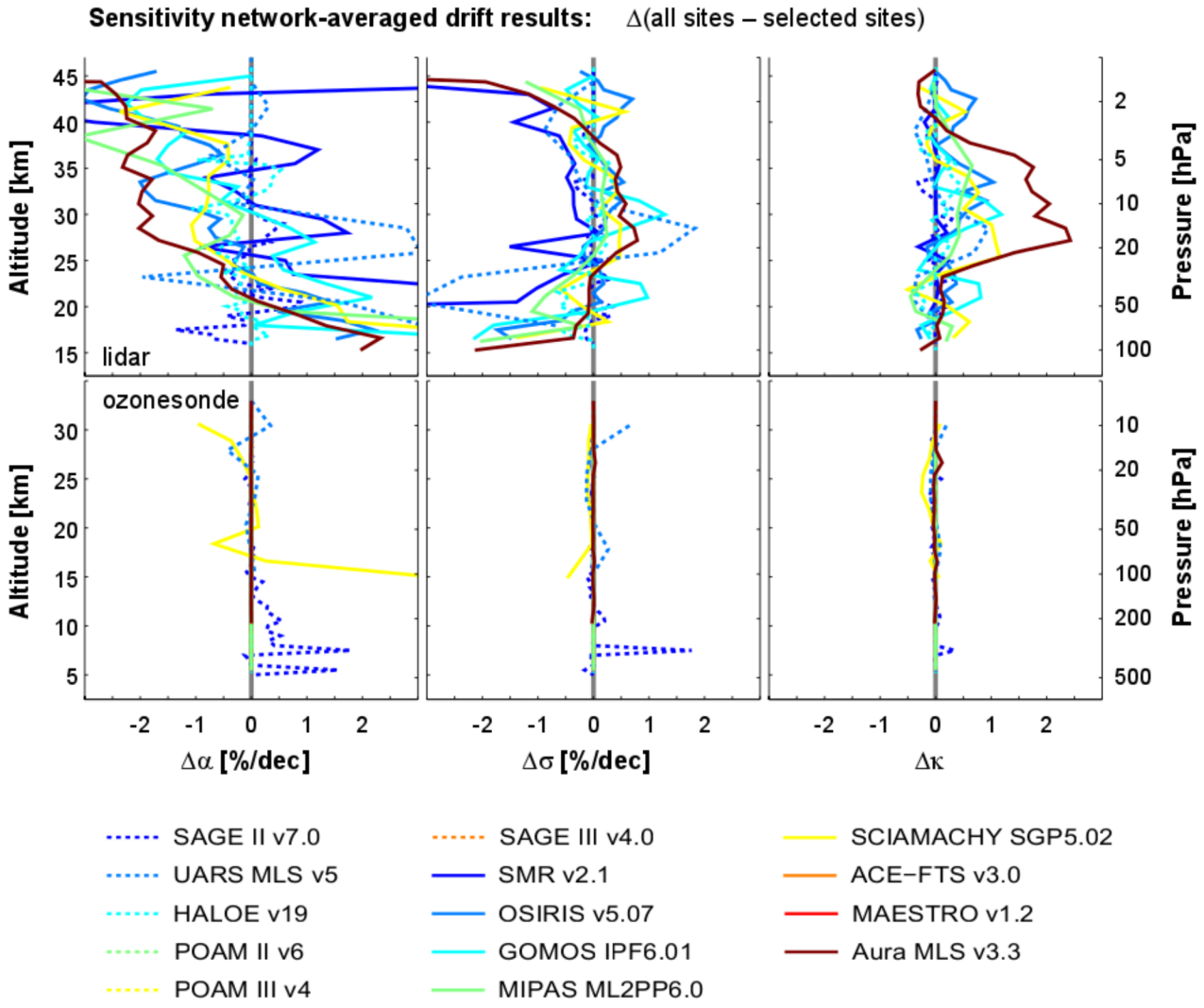

Figure S4. Sensitivity of ozonesonde (bottom) and lidar (top) network-averaged drift 有 one sigma uncertainty 淪 and □-adjustment factor to the selection of ground sites (cfr. Sec. 4.2, Tables 1 and 2). Shown is the difference of the result obtained for the entire ground network minus the result for the selected sites, for the fourteen satellite records.

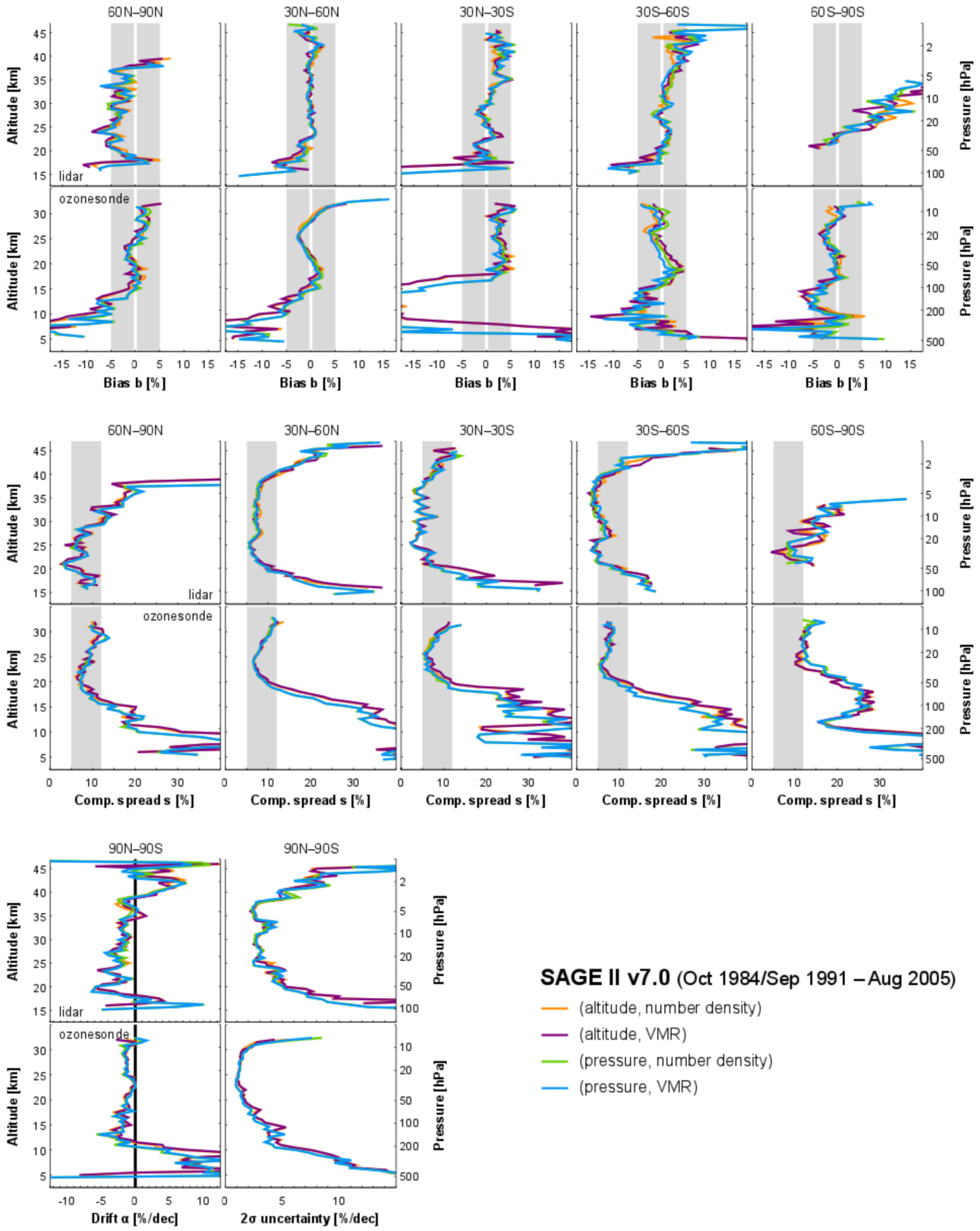

Figure S5. SAGE II v7.0 ozone data quality in different profile representations (see legend): bias (top part), comparison spread (middle) and drift (bottom) from comparisons to NDACC/GAW/SHADOZ ozonesonde and NDACC stratospheric lidar instruments. Only latitude bands with at least 10 comparison pairs are shown. The nominal representation of SAGE II is ozone number density on fixed altitude levels. Satellite and ozonesonde profiles are converted using auxiliary information included in the ozone data files, lidar profiles are converted using ERA-Interim fields. More information in Sect. 6. The SAGE II versus lidar results shown here cover 1991–2005, since we had no ERA-Interim data at our disposal to cover the earlier years. The SAGE II versus ozonesonde results cover 1984–2005.

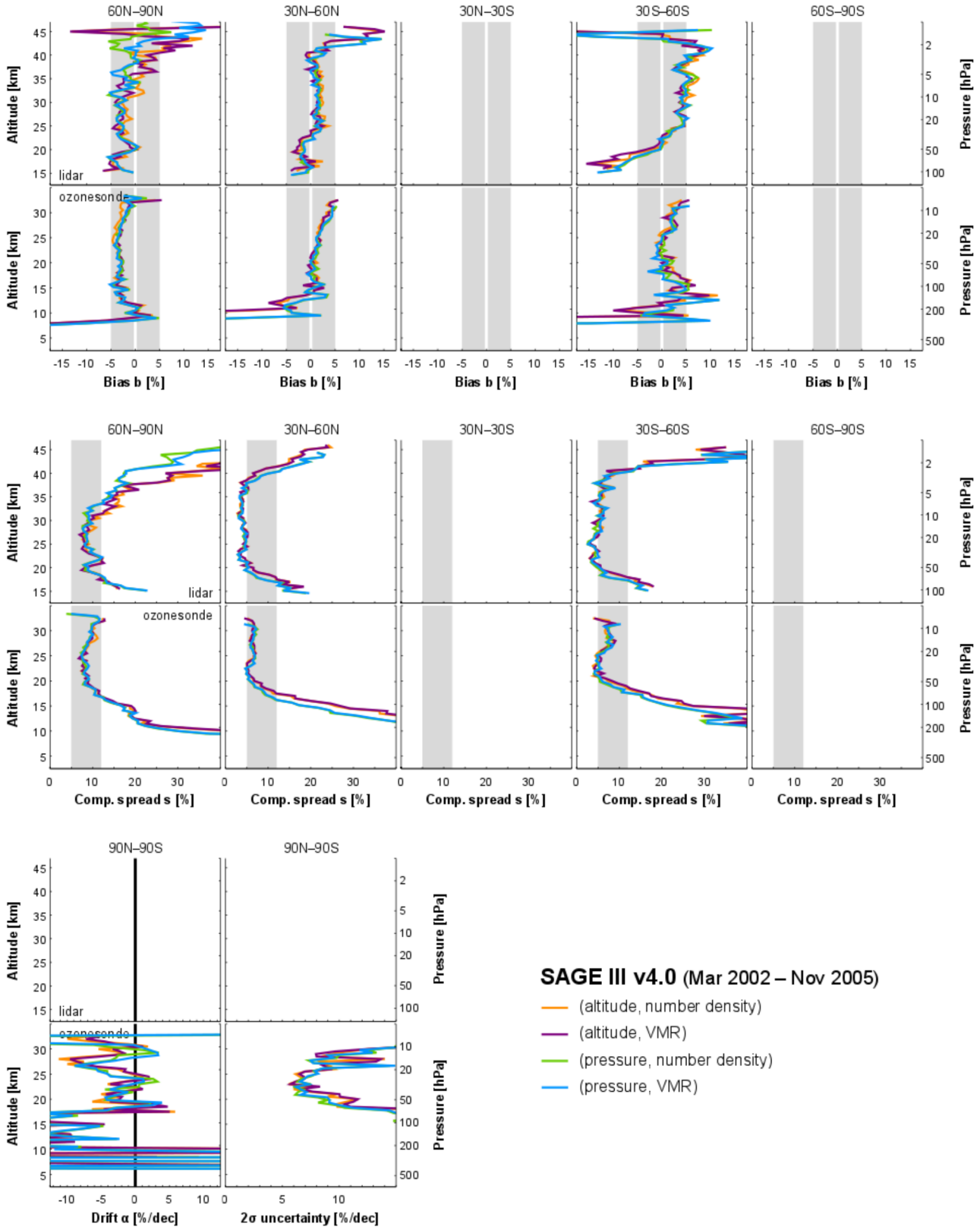

Figure S6. Same as Fig. S5, but for SAGE III v4.0 (nominal representation: ozone number density on fixed altitude levels).

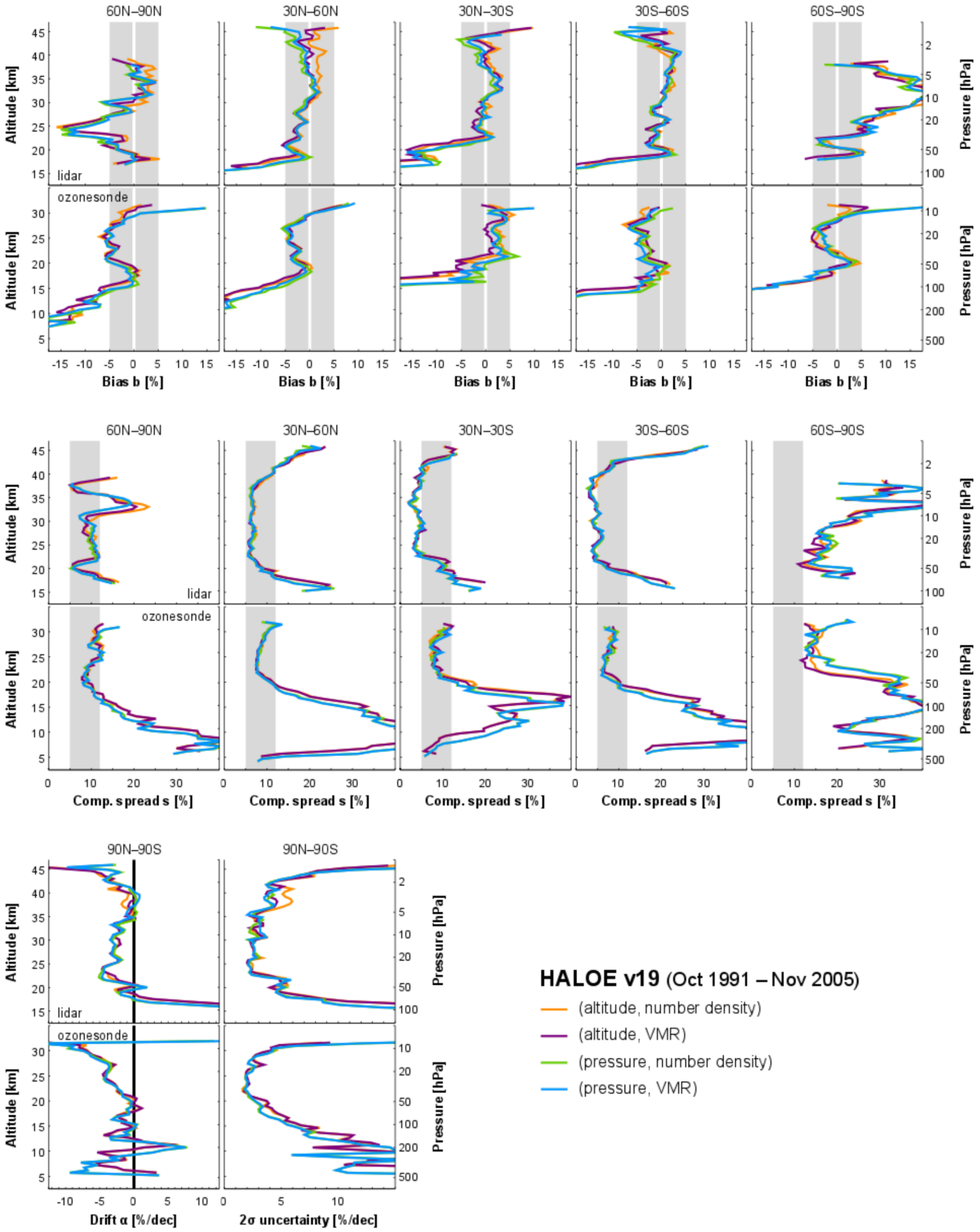

Figure S7. Same as Fig. S5, but for HALOE v19 (nominal representation: ozone VMR on fixed pressure levels).

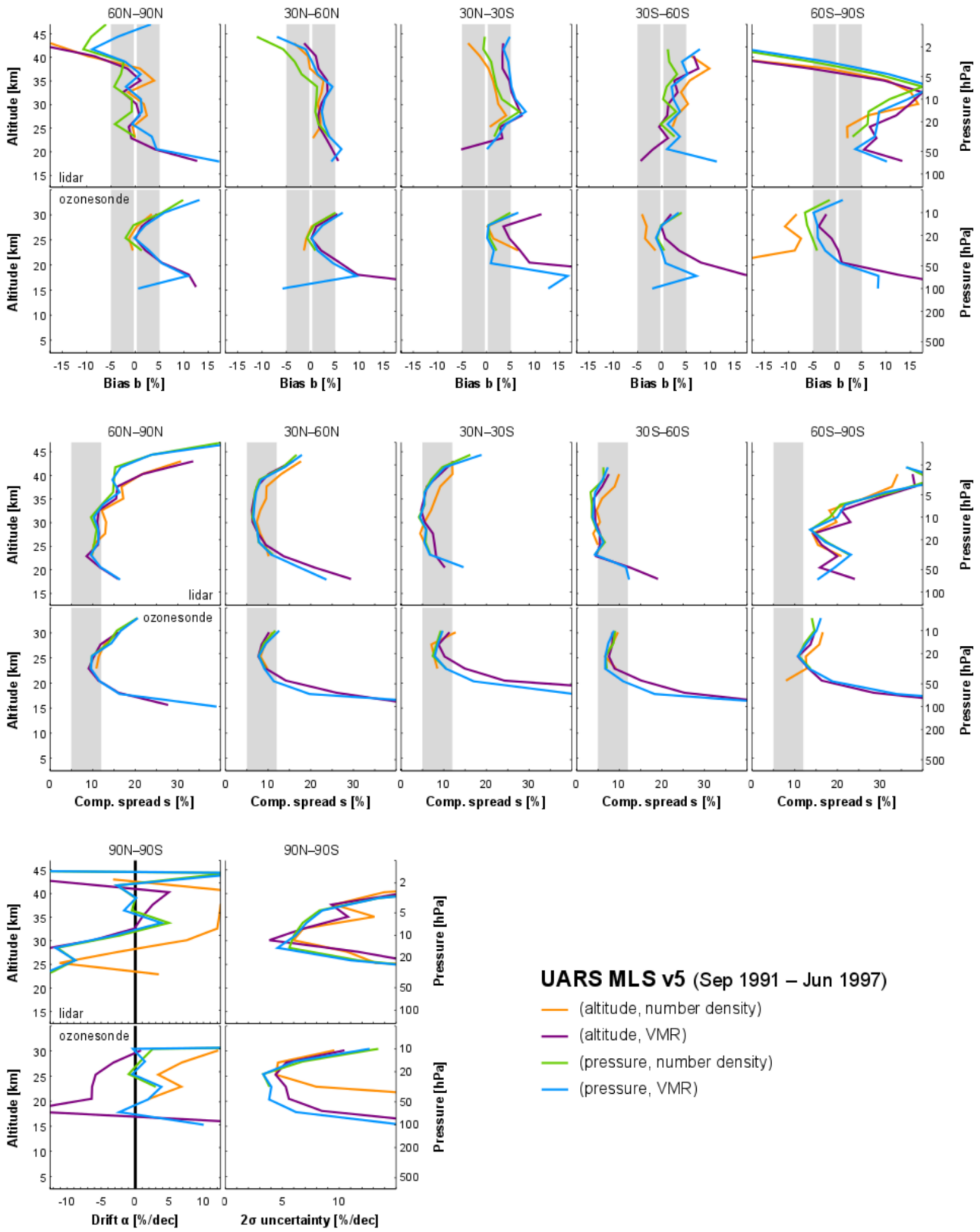

Figure S8. Same as Fig. S5, but for UARS MLS v5 (nominal representation: ozone VMR on fixed pressure levels).

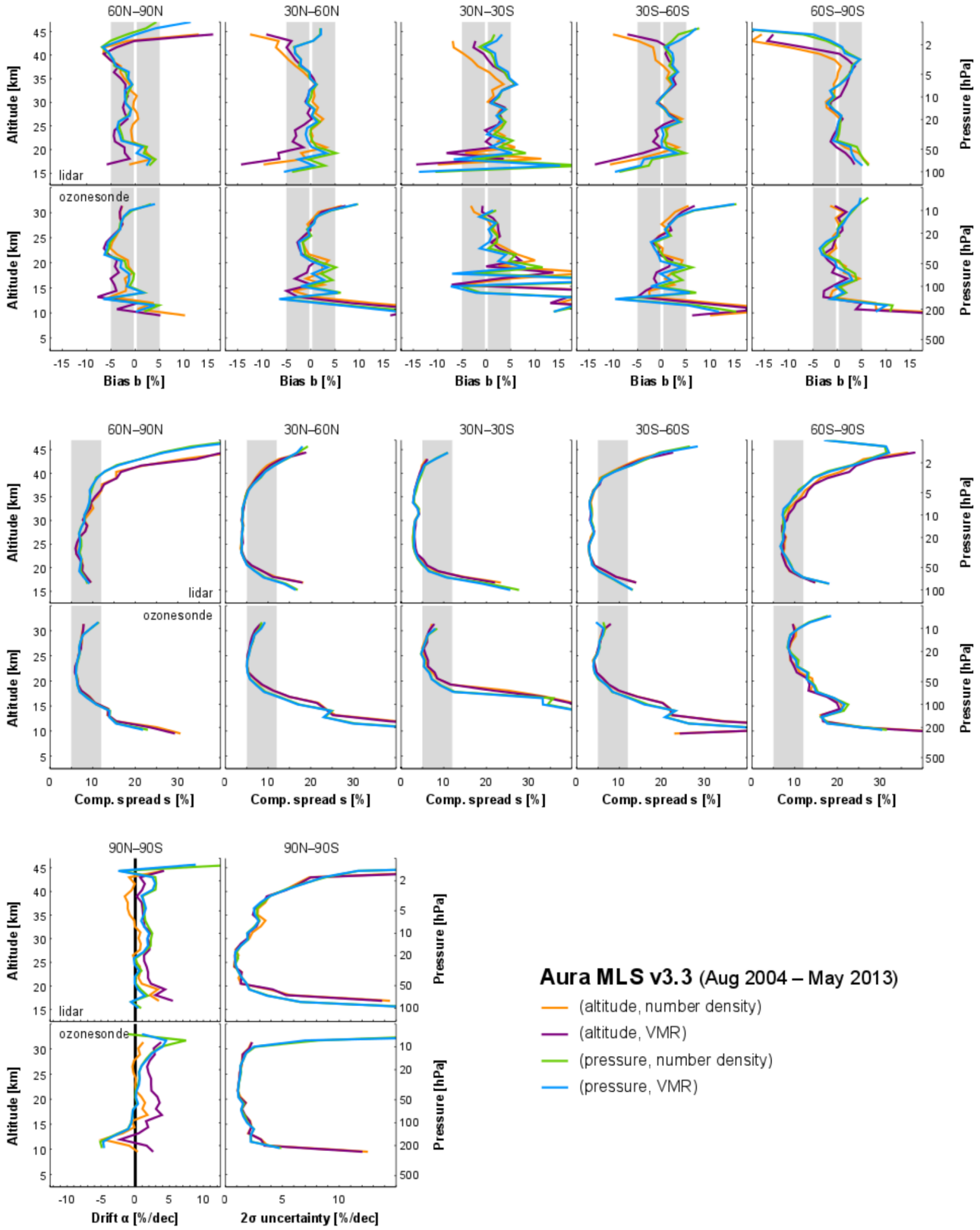

Figure S9. Same as Fig. S5, but for Aura MLS v3.3 (nominal representation: ozone VMR on fixed pressure levels).

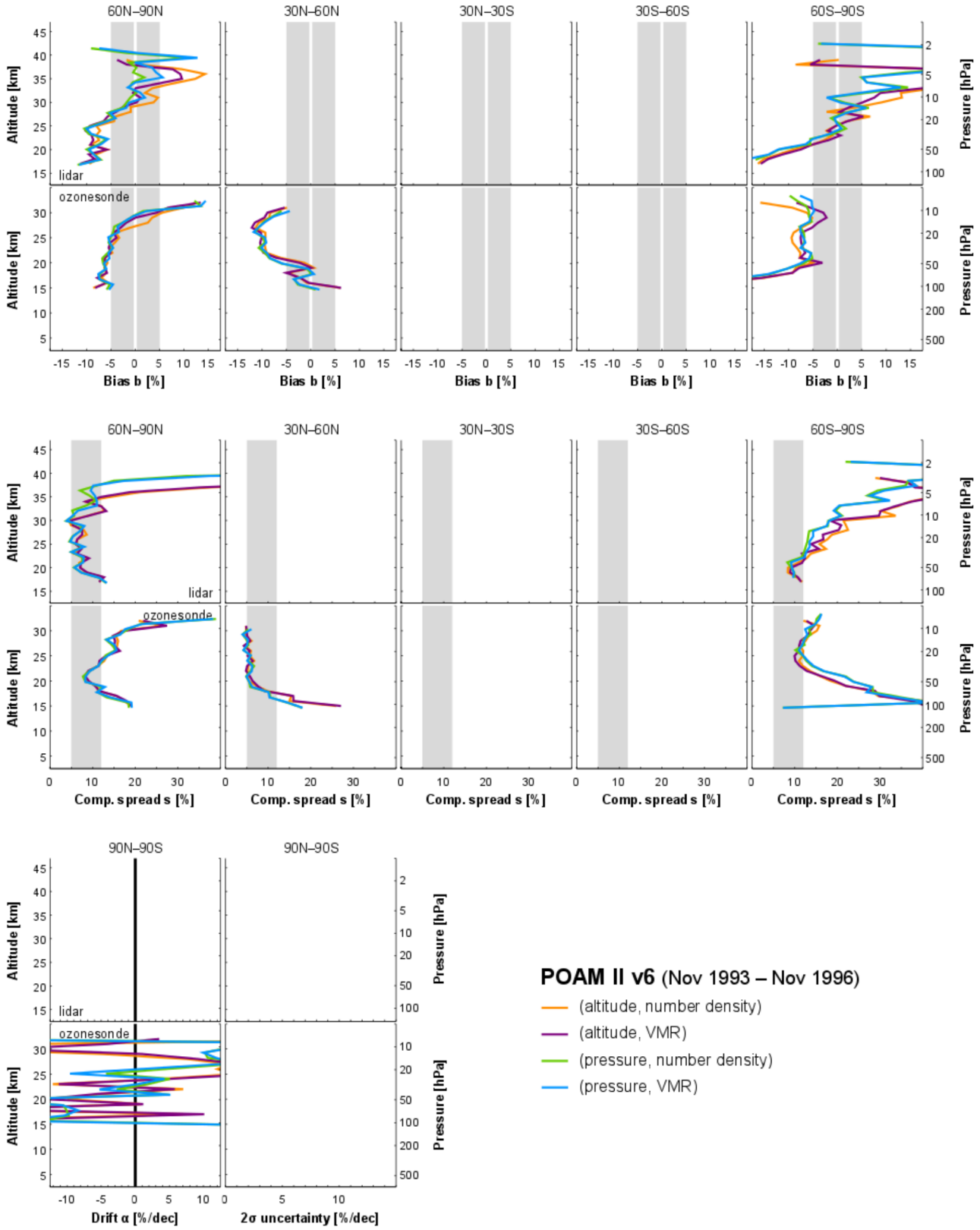

Figure S10. Same as Fig. S5, but for POAM II v6 (nominal representation: ozone number density on fixed altitude levels).

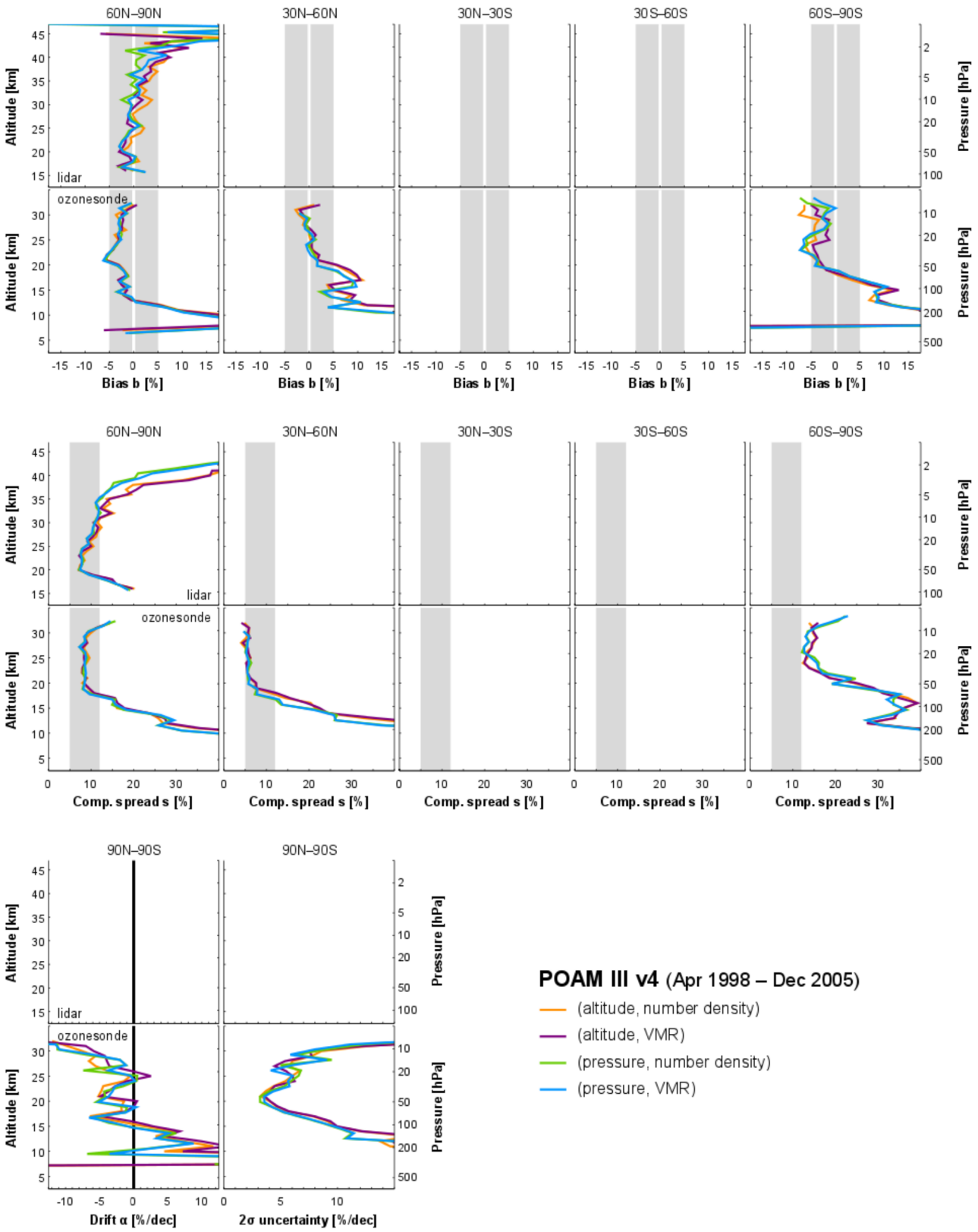

Figure S11. Same as Fig. S5, but for POAM III v4 (nominal representation: ozone number density on fixed altitude levels).

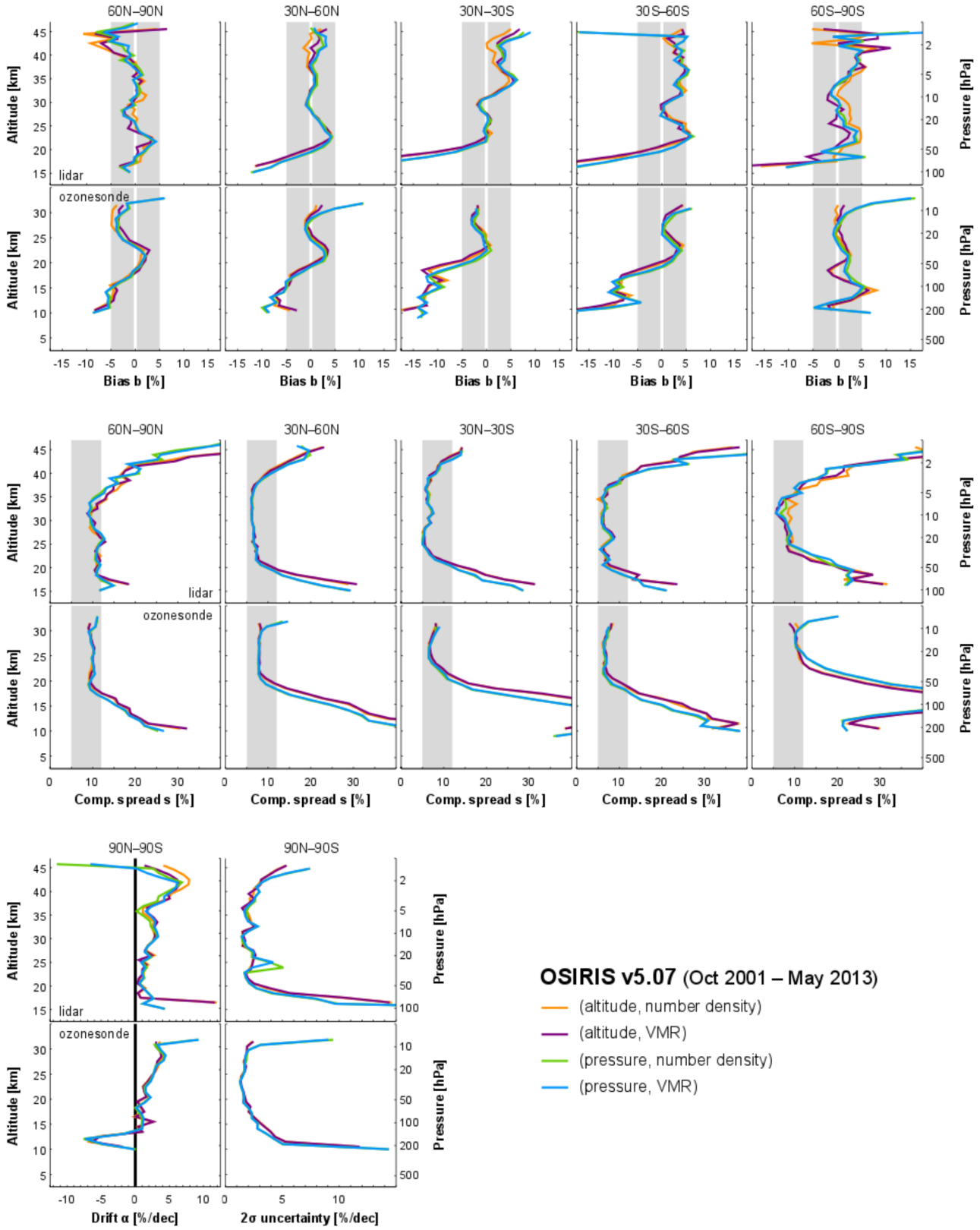

Figure S12. Same as Fig. S5, but for OSIRIS v5.07 (nominal representation: ozone number density on fixed altitude levels).

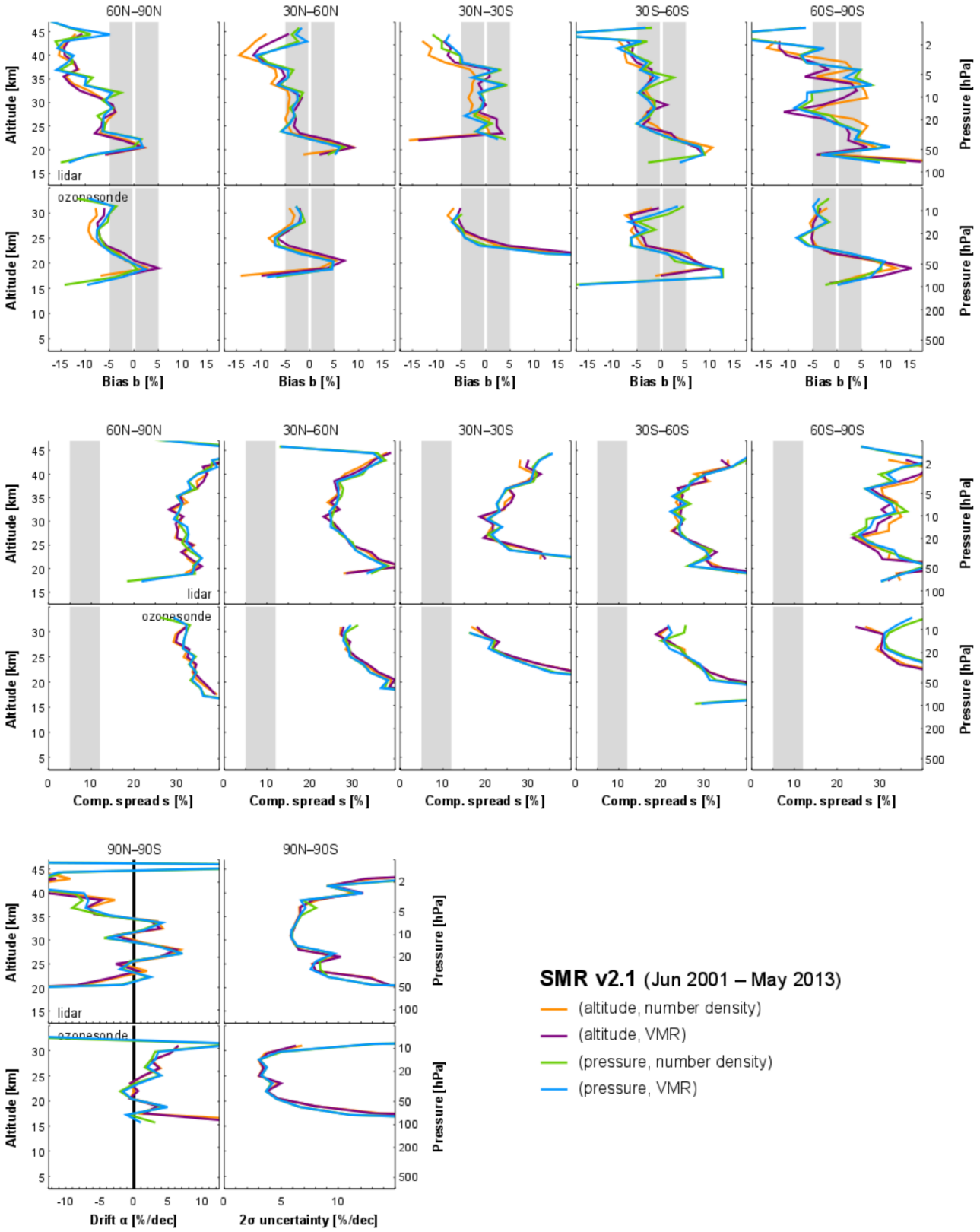

Figure S13. Same as Fig. S5, but for SMR v2.1 (nominal representation: ozone VMR on variable altitude levels).

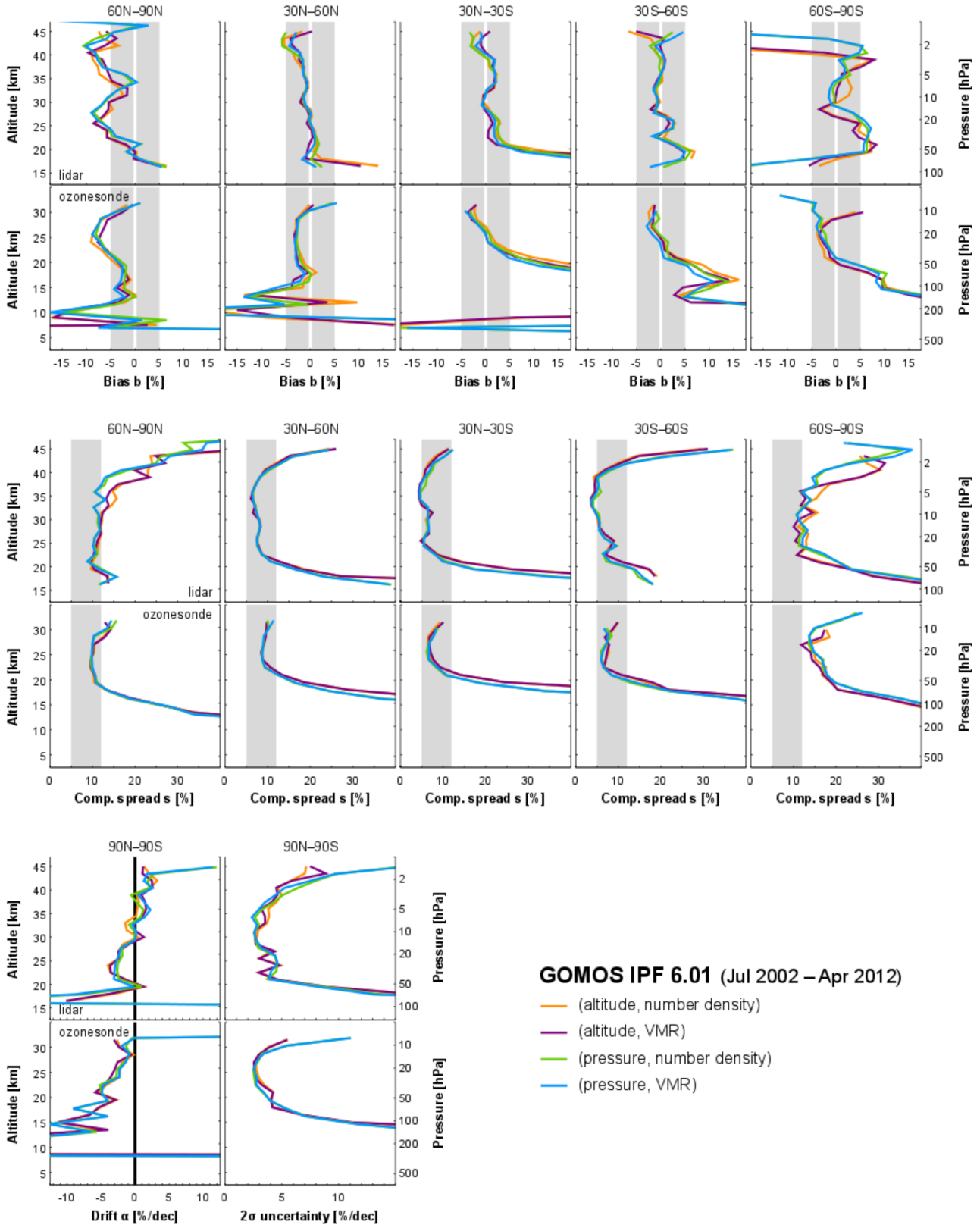

Figure S14. Same as Fig. S5, but for GOMOS IPF6.01 (nominal representation: ozone number density on variable altitude levels).

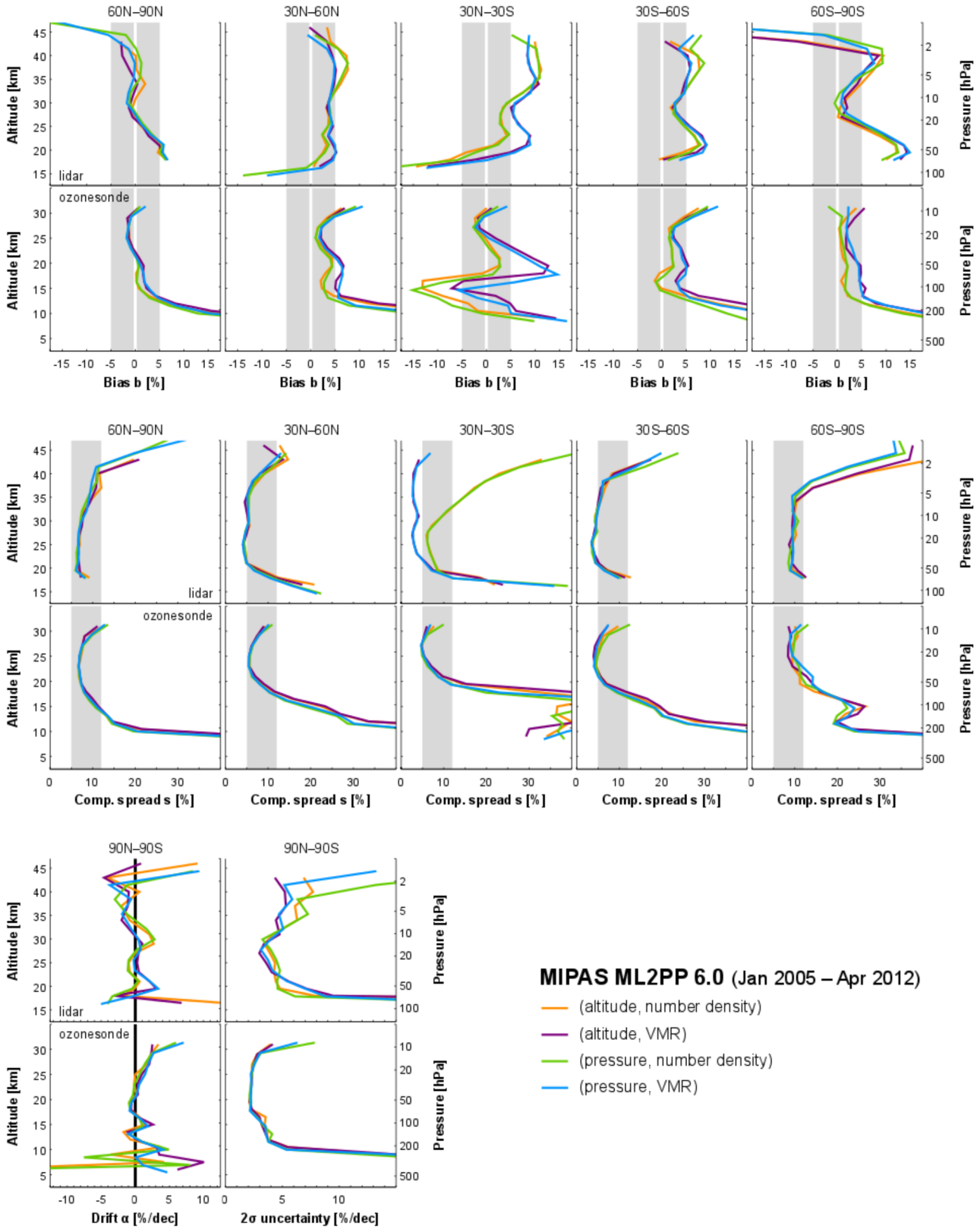

Figure S15. Same as Fig. S5, but for MIPAS ML2PP6.0 2005–2012 nominal observation data (nominal representation: ozone VMR on variable pressure levels). The large increase in the spread of tropical lidar comparisons is due to outliers in the averaging kernels. It is not seen when a triangular smoothing function is used.

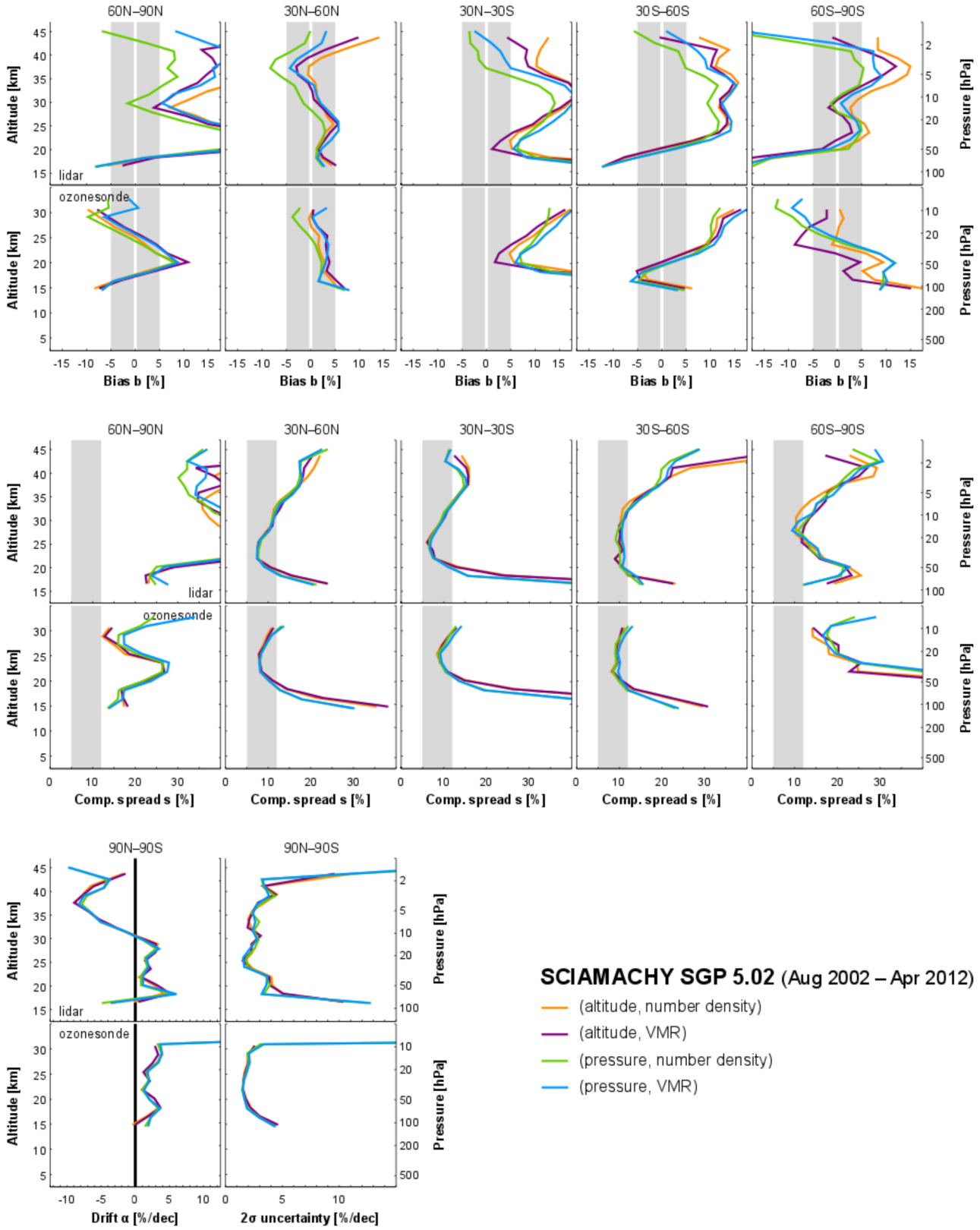

Figure S16. Same as Fig. S5, but for SCIAMACHY SGP5.02 (nominal representation: ozone number density on fixed altitude levels).

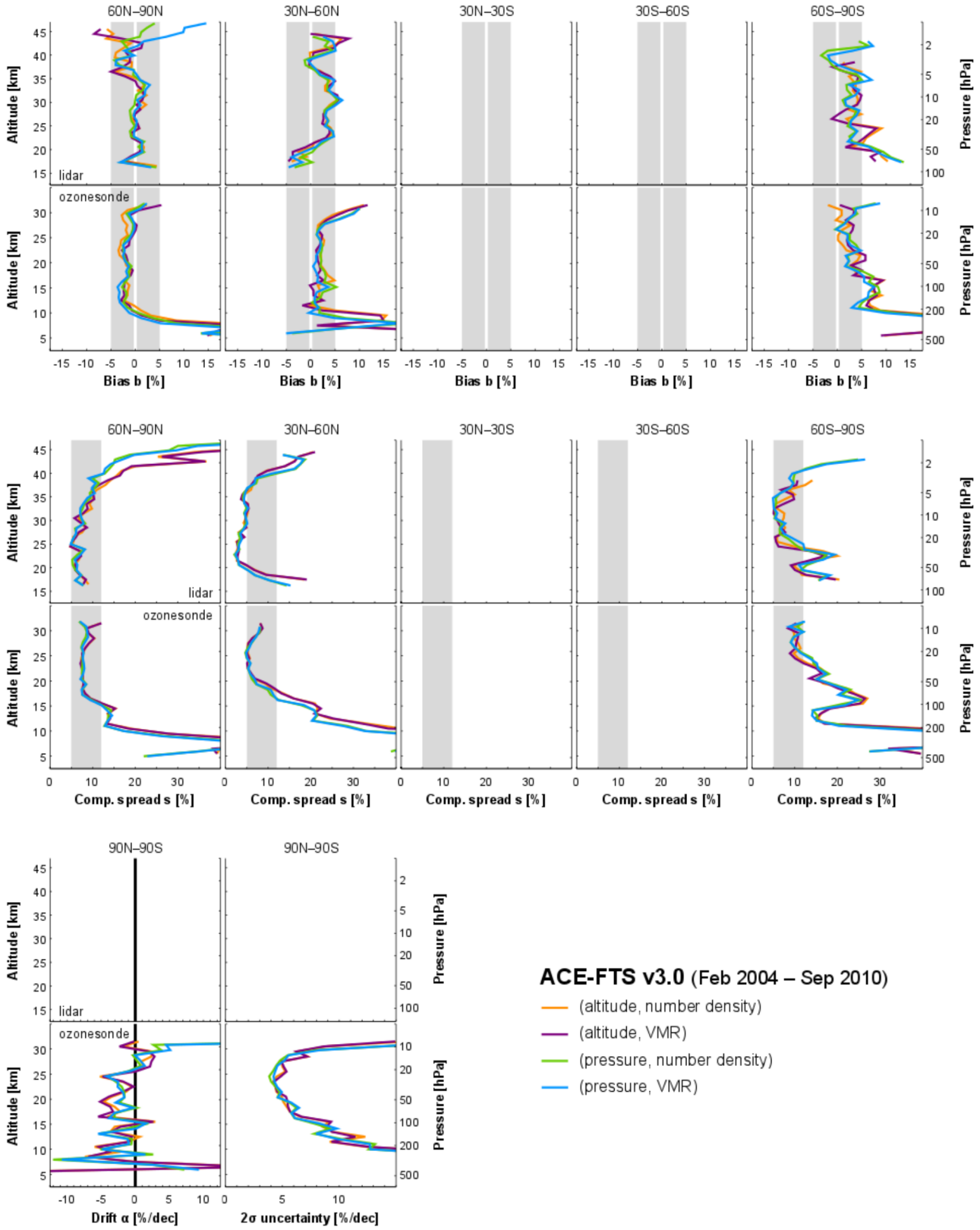

Figure S17. Same as Fig. S5, but for ACE-FTS v3.0 (nominal representation: ozone VMR on fixed altitude levels).

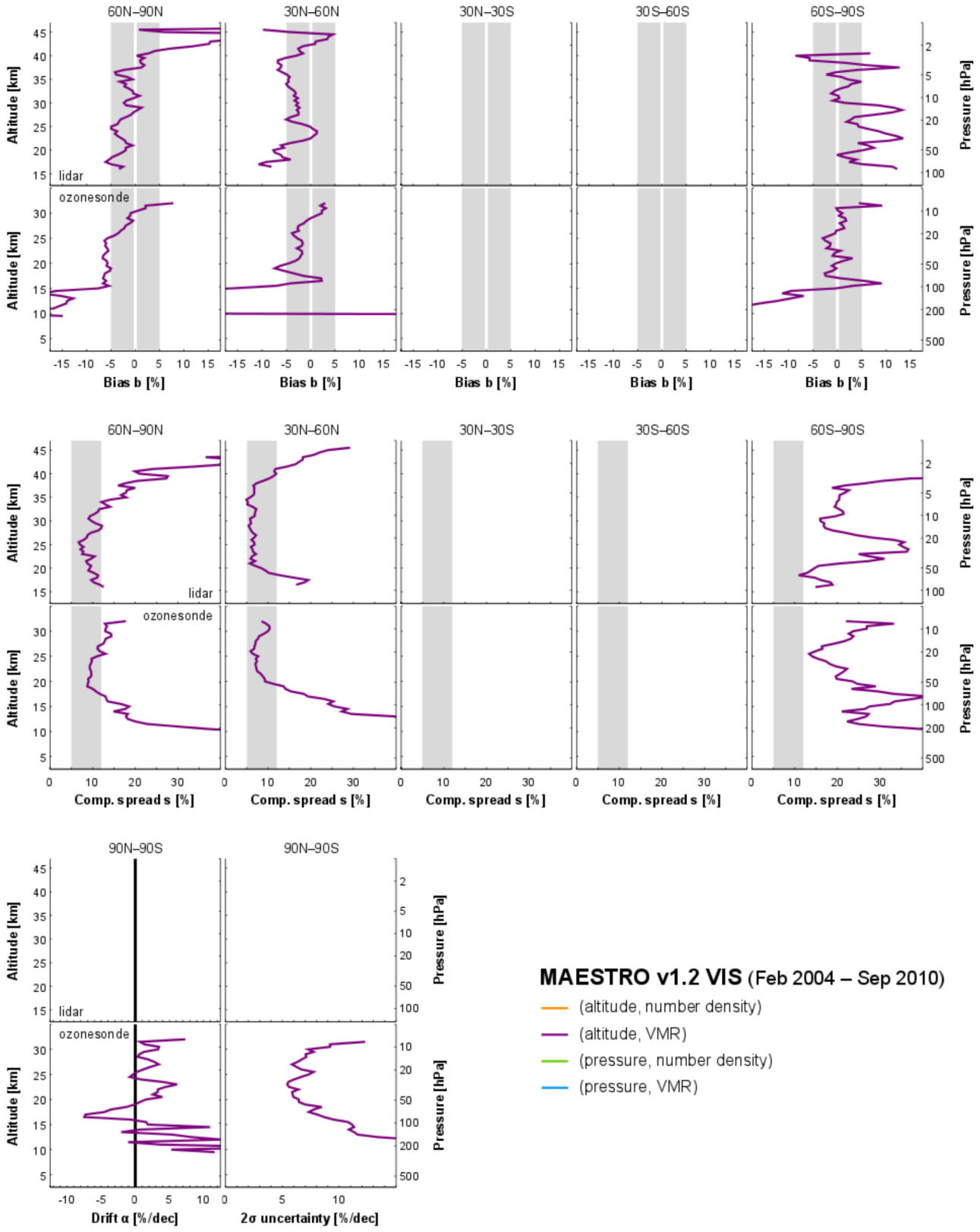

Figure S18. Same as Fig. S5, but for the nominal representation of MAESTRO v1.2 (ozone VMR on variable altitude levels). Non-native representations were not verified here since the required auxiliary data are identical to those of ACE-FTS v3.0. So we expect a similar representation-dependence as in Fig. S17.

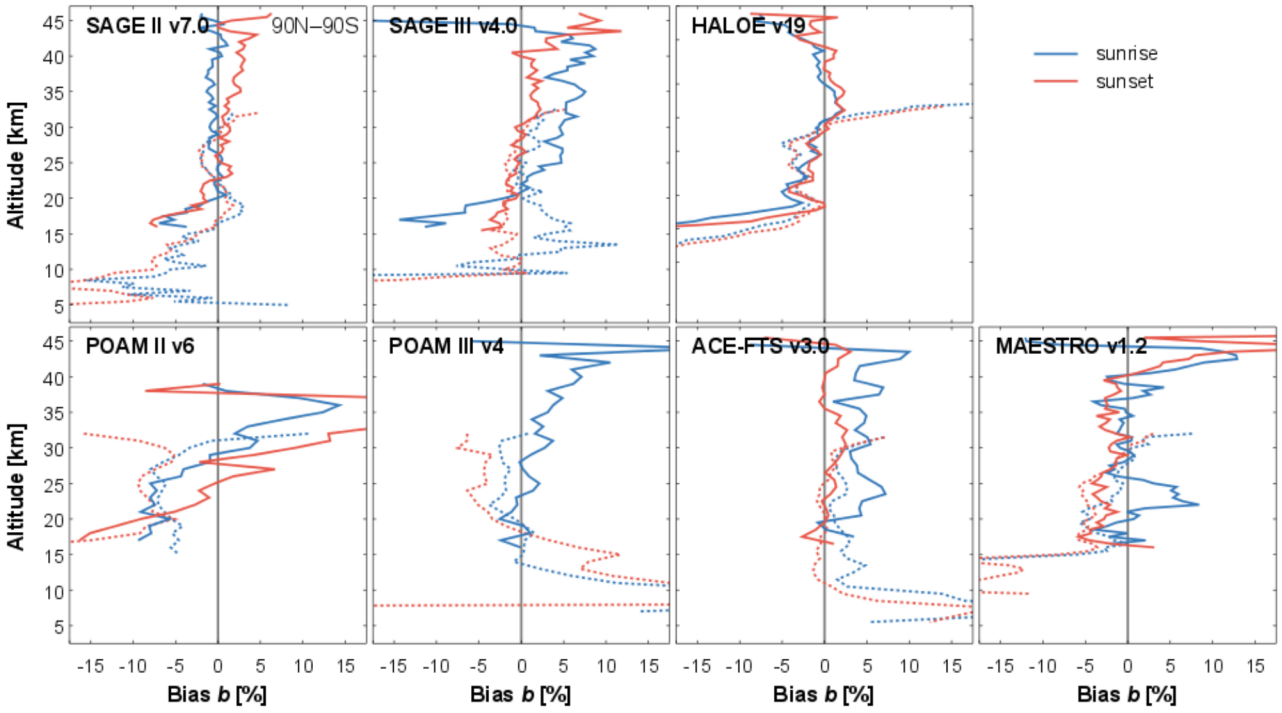

Figure S19. Bias relative to ozonesonde (dashed) and lidar (solid) of the sunrise and sunset measurements by seven solar occultation instruments. The bias is calculated over the entire ground-based network. The analysis is performed in the native profile representation of each satellite record.

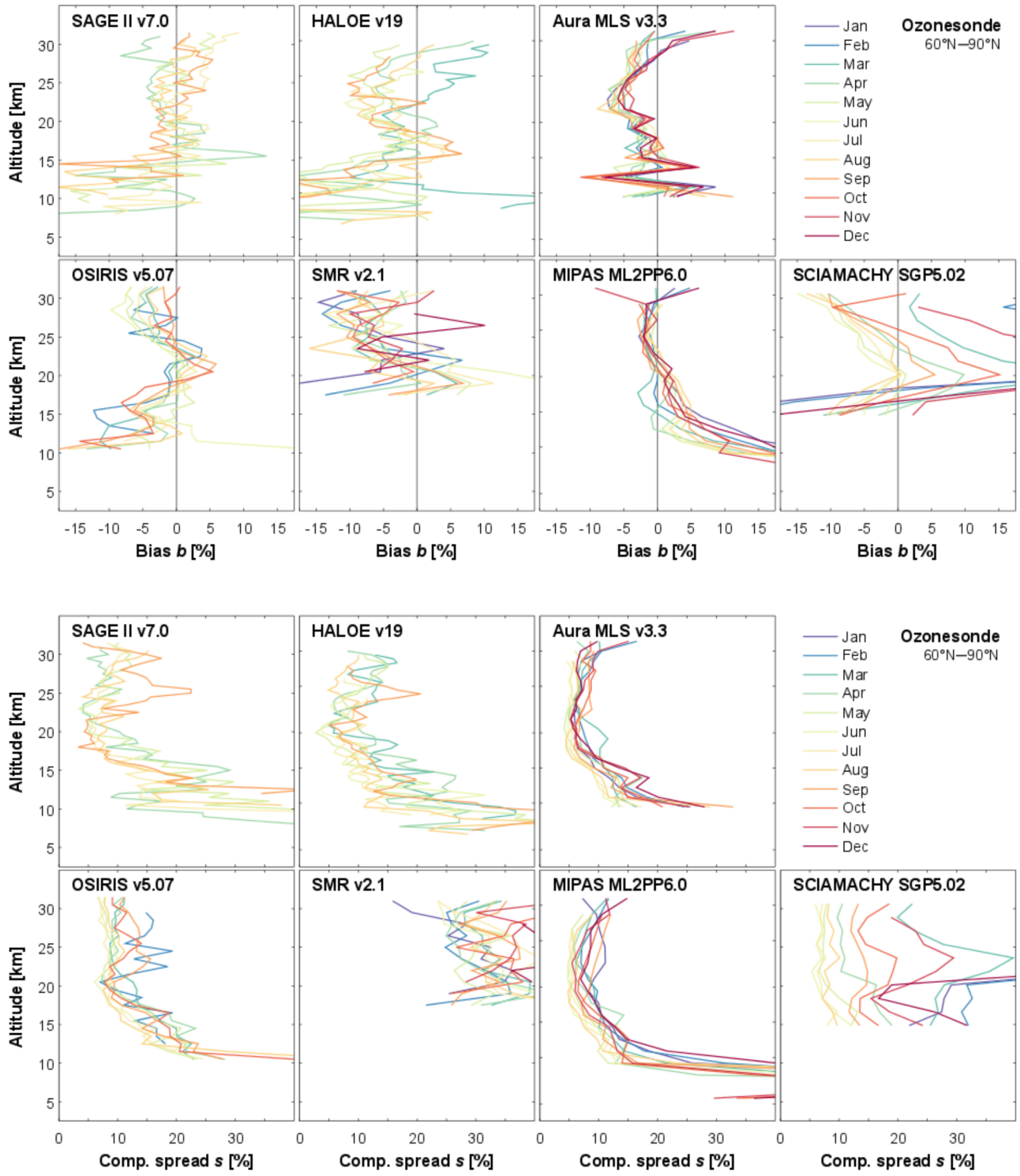

Figure S20. Dependence on month of the bias (top part) and spread (bottom) for comparisons of seven satellite records to Arctic ozonesonde data. The analysis is performed in the native profile representation of each satellite record.